Optimal Coil Size Ratios for Wireless Power Transfer Applications

Benjamin H. Waters[1], Brody J. Mahoney[1], Gunbok Lee[2] and Joshua R. Smith[1]
[1]Dept. of EE and CSE, University of Washington, Seattle, WA 98195, USA
[2]Dept. of EE, Pohang University of Science and Technology, Pohang, Gyungbuk, 790-784, Korea
Email: bhw2114@uw.edu

***Abstract*—Optimization of coil sizes for wireless power transfer applications has a significant impact on the range and efficiency of the wireless power system. Often it is difficult to accurately analyze how a set of coils will perform before they are constructed due to the complexity of approximating the parasitic components and coupling coefficients associated with the coils. Also, for certain wireless power applications such as consumer electronic devices, implanted medical devices and industrial equipment that have physical constraints on the size and shape of the coils, it can be a difficult and time-consuming process to design and evaluate several different coil configurations for optimal range and efficiency. This paper provides simplified design equations to accurately calculate the self inductance, capacitance, resistance, quality factor and coupling coefficient in terms of coil geometries for flat, spiral coils. Experimental results validate the analysis and a design example is provided to optimize the size of a transmit coil for maximum range and wireless power efficiency to a 5.8cm receive coil used in a four-element wireless power transfer system.**

I. Introduction

The growing number of wireless power transfer (WPT) applications demand highly efficient WPT at ranges well beyond those of commercially available wireless charging pads, which require physical contact between the transmit (Tx) and receive (Rx) coil. The successful implementation of contactless wireless power hinges on convenience for the user and compliance with safety and regulatory standards. Maximizing WPT efficiency enables lower transmitted power, thereby decreasing the field strength of emissions, maintaining low coil temperatures, and facilitating regulatory compliance for any application.

Two critical parameters for long range and highly efficient WPT between two coils are the quality factor Q for each coil and the coupling coefficient k between the coils. High Q and stronger k between two coils results in greater efficiency at a longer WPT range [1]. However, high Q does not necessarily imply high k, especially if the Tx and Rx coils are not equally sized. The size and geometry of the Tx and Rx coils significantly impact both Q and k independently.

In this work, a flat, spiral multi-turn coil topology is considered due to the wide range of applications that can physically accommodate such a coil. Extensive prior work has provided expressions for the inductance L, resistance R, and capacitance C for lumped modeling of flat spiral coils in terms of the coil geometry [2], [3], [4], and outlined optimization techniques for coil design using Litz wire to minimize the skin effect [5] and for biomedical applications [6]. However, these expressions and techniques are typically complex, computationally intensive, and can be inaccurate for a wide range of coil sizes and operating frequencies. Other work has shown how to calculate the coupling coefficient between two flat spiral coils [7]. However few articles demonstrate the effects that the coil size has on both Q and k, and the overall impact on WPT range and efficiency.

In this work, we provide simplified expressions for Q and k in terms of the coil geometry for a flat, spiral coil. We experimentally validate these expressions and prove their accuracy under certain geometric constraints. Using these expressions, we determine the optimal ratio of the transmit coil outer diameter to receive coil outer diameter $\frac{D_{O,TX}}{D_{O,RX}}$ that results in the highest efficiency at the longest range. We provide an example that uses this technique to design Tx and Rx coils that maximize efficiency across a targeted distance range for the desired application given only the maximum allowable size of each coil.

II. Design Equations

Expressions for L, R, C, Q, and k of flat spiral coils are solved in terms of the outer diameter D_o, number of turns N, spacing between each turn p and wire diameter w of the coil. Although D_O, N, p and w fully define a flat, spiral coil, all geometric parameters are shown for completeness in Fig. 1. The inner diameter D_i, total wire length l, winding radius a, and radial depth of the winding c are defined in (1) and (2). All units of length are in meters.

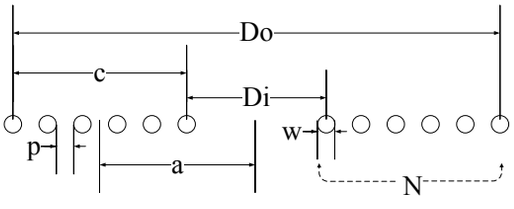

Fig. 1. Cross-sectional view of flat spiral coil.

$$D_i = D_o - 2N(w+p), \qquad l = \frac{1}{2}N\pi(D_o + D_i) \quad (1)$$

$$a = \frac{1}{4}(D_o + D_i), \qquad c = \frac{1}{2}(D_o - D_i) \quad (2)$$

978-1-4799-3432-4/14/$31.00 ©2014 IEEE

A. Inductance

The self inductance for flat, spiral coils is shown in (3). L is derived from a modification of Wheeler's formula for a single-layer helical coil, while accounting for the conversion from inches to meters ($39.37\frac{in.}{m}$) and μH to H (10^{-6}) [3].

$$L(H) = \frac{N^2(D_o - N(w+p))^2}{16D_o + 28N(w+p)} \times \frac{39.37}{10^6} \tag{3}$$

The inductance expression is validated in prior work for a wide variety of coils and found to be accurate for most geometries except when the coil has very few turns, when the pitch is very large relative to the wire diameter ($p >> w$), and when $\frac{c}{a} < 0.2$ [3]. Since these boundary conditions typically correspond to low inductance (i.e. low Q for a series resonator) and the goal for WPT is high Q, the conditions that would lead to inaccuracy in (3) are typically inapplicable when designing WPT coils.

B. Capacitance

The self capacitance of a spiral coil depends on the relative permittivity of the conductor, the diameter of each turn, the number of turns, and the pitch. As the number of turns increases, the self capacitance becomes increasingly difficult to calculate accurately due to the nonlinear adjacent winding capacitance [4]. Typically, the self capacitance is on the order of a few pF, and is small compared to the required tuning capacitor for resonance at 13.56MHz. Therefore, the required tuning capacitance of the coil is defined in terms of the inductance and resonant frequency f as in (4) and the parasitic self capacitance is neglected for this simplified expression.

$$C(F) = \frac{1}{(2\pi f)^2 L} \tag{4}$$

C. Resistance

Power loss in a spiral coil consists of radiation and conduction losses. Typical WPT coils are relatively small compared to the operating wavelength (∼22m at 13.56MHz). Thus conduction loss is the dominate loss mechanism, while radiation loss is typically negligible. Conduction loss is dependent on the skin effect and proximity effect. Both effects confine current flow to smaller cross-sectional areas through the conductor, which increases the effective resistance of the conductor [2].

For spiral coils, the parameter that contributes most to fluctuations in total resistance R is the pitch p. Because of the proximity effect, R is inversely proportional to p, and this effect is nonlinear. For tightly wound coils, accurate expressions for R that account for the proximity effect are complex and can be difficult to calculate [2]. For loosely wound coils, the proximity effect can be negligible, so R consists of only the DC resistance R_{DC} and the skin depth δ, which can be approximated with a simpler expression shown in (6) where μ_0 is the permeability of free space and σ is the conductivity of the conductor ($\sigma = 59.6 \times 10^6 \frac{S}{m}$ for copper). At 13.56MHz, $\delta = 17.7\mu$m and is much smaller than the wire diameter ($\simeq$ 1mm) for the coils investigated in this analysis. So (6) has been derived from the very high frequency model of AC resistance from Kaiser [8].

$$R_{DC} = \frac{l}{\sigma\pi(w/2)^2}, \quad \delta = \frac{1}{\sqrt{\pi f \sigma \mu_o}} \tag{5}$$

$$R = R_{DC}\frac{w}{4\delta} = \sqrt{\frac{f\pi\mu_o}{\sigma}}\frac{N(D_o - N(w+p))}{w} \tag{6}$$

D. Quality Factor

Using the L, C and R expressions from (3), (4), and (6) respectively, Q is defined as follows for the series resonant flat spiral coil:

$$Q = \frac{1}{R}\sqrt{\frac{L}{C}} = \frac{39.37}{10^6}\sqrt{\frac{f\pi\sigma}{\mu_o}}\frac{wN(D_o - N(w+p))}{8D_o + 14N(w+p)} \tag{7}$$

This expression can be used to optimize coil design for high Q and ensure resonance at the desired operating frequency.

E. Coupling Coefficient

The amount of magnetic flux generated by the Tx coil which passes through the Rx coil determines k. Typically k depends on the geometries of each coil, the distance between the coils, and the relative orientation of the coils. The full expression for k between two single-turn loops can be simplified by assuming the loops are always oriented with zero angular misalignment between them [7]. Using this simplified expression for k and summing over the i^{th} turn from the Tx coil and the j^{th} turn from the Rx coil, the mutual inductance M between two multi-turn spiral coils is simplified to

$$M = \sum_{i=1}^{N_{TX}}\sum_{j=1}^{N_{RX}} \mu_o R_i R_j \int_0^{\pi} \frac{cos(\Theta)d\Theta}{\sqrt{{R_i}^2 + {R_j}^2 + d^2 - 2R_iR_jcos(\Theta)}} \tag{8}$$

where d is the separation distance between the Tx and Rx coils, R_i and R_j are the corresponding radii of each turn for the Tx and Rx coils respectively, and k is related to M by

$$k = \frac{M}{\sqrt{L_i L_j}}. \tag{9}$$

Evaluating (8) shows that maximum k occurs for two coils of equal size. However, k diminishes faster with increasing distance between symmetrical coils. Since most WPT applications consist of asymmetrical coil sizes, it is necessary to optimize Tx and Rx coil geometries to achieve maximum Q without diminishing k.

F. Validation of Coil Parameters

The expressions for L and R shown in (3) and (6) respectively are validated against measured results for eight different test coils shown in Fig. 2. Each test coil has the same $D_o = 8$cm, $D_i = 0$, $w = 1.024$mm, $f = 13.56$MHz; however, the pitch and number of turns for each coil are different and are listed in Fig. 2. The measured values of L and R for each test coil were evaluated by extracting S_{11} from an HP8753

vector network analyzer (VNA) and using a best-fit analysis to match L, R, and C to the equivalent circuit model for a series resonant coil with input impedance Z_{IN} shown in (10).

$$Z_{IN} = R + j\omega L + \frac{1}{j\omega C}, \qquad S_{11} = \frac{Z_{IN} - 50\Omega}{Z_{IN} + 50\Omega} \tag{10}$$

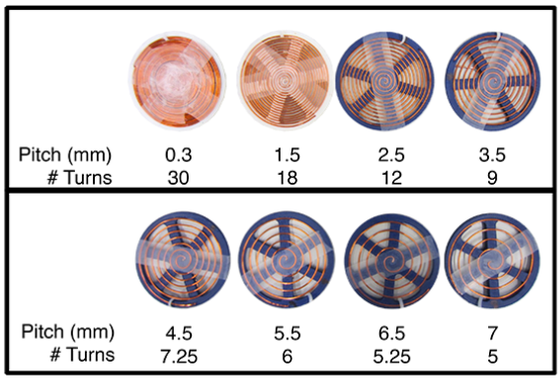

Fig. 2. Coils used for validation of parasitic component calculations.

The results for the measured and calculated L and R are plotted in Fig. 3. The inductance calculation is accurate for both tightly and loosely wound coils. For resistance, the proximity effect model using the AC resistance calculation from [2] is more accurate for tightly wound coils, but over-approximates R for larger p. The skin effect model from (6) underestimates R for tightly wound coils, but is more accurate for $p > 2.5$mm (approximately 2.5 times greater than the wire diameter of 1.024mm). Since R increases exponentially for tightly wound coils, and high Q requires low R, it is preferable to design coils that are not tightly wound for WPT applications. Therefore (6) will be used for the remainder of this analysis to calculate R with the constraint that $p > 2.5w$.

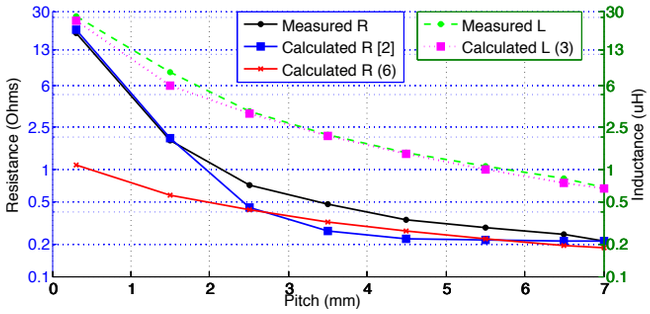

Fig. 3. R and L vs. p for the eight test coils from Fig. 2. The first R calculation result accounts for both proximity effects and skin effects [2] while the second calculation accounts for only the skin effect and DC resistance (6).

III. Simulation and Experimental Results

The analysis for Q and k from Section II will be used to show how the Tx and Rx coil geometries impact both range and efficiency for a 4-element WPT system. The schematic of a 4-element WPT system is shown in Fig. 4. This system consists of a Tx loop, Tx coil, Rx coil, and Rx loop. Each coil is magnetically coupled to the subsequent coil by coupling coefficients k_{12}, k_{23}, and k_{34} respectively. The transfer function for a 4-element WPT system is not shown here, but can be found in prior work [1].

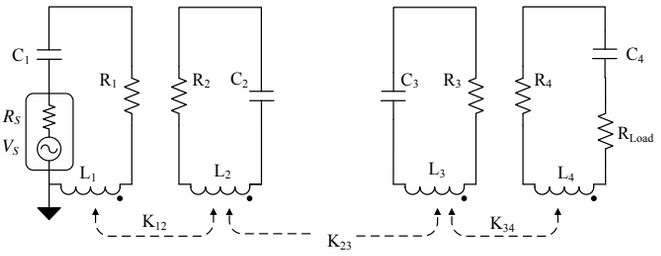

Fig. 4. Schematic of a four-coil WPT system.

Although a design example using a 4-element WPT system is outlined here, the following analysis can be generalized to a 2, 3, or n-element WPT system by using the transfer function for the desired WPT system. The results from this design example are plotted in Fig. 5. However, the following procedure can be used for any Tx and Rx coil size, provided the expressions for L, R, and C of the coils are accurate for the specified range of coil geometries.

1) Define the maximize allowable Rx coil size. For the example used in this procedure, $D_{O,RX,max} = 5.8$cm.
2) Define a range of allowable Tx coil sizes. In this example, 2cm$<D_{O,TX}<$90cm has been selected.
3) Maximize Q using (7) for each Tx coil size and the Rx coil by exhaustively evaluating all possible combinations of p and N for which the expressions have known accuracy. The constraints from Section II include $p > 2.5w$, $D_i > 0$, and $f = 13.56$MHz. In this example, $Q_{RX,max} = 520.9$ for the $D_{O,RX} = 5.8$cm Rx coil using $N = 6$, $p = 2.56$mm, and 18AWG copper wire ($w = 1.03$mm).
4) Using the geometries for each optimized Tx coil, calculate the achievable k_{23} for a range of distances targeted by the application. In this example, $0<d<140$cm has been selected as the ideal operating range. The goal is to maximize efficiency across this entire distance range.
5) Using k_{23}, $Q_{RX,max}$ and Q for each Tx coil, select Q of the Tx and Rx loops, k_{12} and k_{34} for an optimal figure of merit as outlined for symmetrical coils in Section IV from [1] or for asymmetrical coils from [9].
6) Using the calculated optimal values for each coil in the 4-element WPT system, evaluate the transfer function shown in Section III from [1] at $f = 13.56$MHz.
7) Select the optimal Tx coil size for maximum efficiency at the longest or desirable range for the intended application. In this example, the results of this analysis are plotted in Fig. 5.

Fig. 5 is divided into two regions where the Tx coil is larger and smaller than the Rx coil. In both regions, $|S_{21}| > 0.9$ can be achieved. The two ridges converge as the distance increases and this high $|S_{21}|$ cannot be achieved as the distance between the coils increases beyond approximately 11mm, which corresponds to a distance of approximately $2D_{O,RX}$. A valley exists at close distances for coils with a ratio close

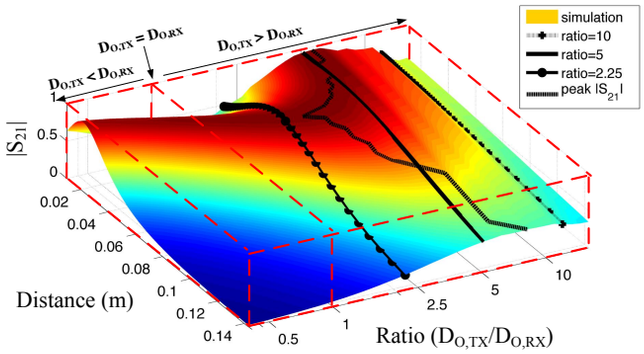

Fig. 5. $|S_{21}|$ as a function of Tx to Rx coil size ratio ($\frac{D_{O,TX}}{D_{O,RX}}$) and distance between the coils.

to one because k is high for similarly sized coils, and in this overcoupled region, high $|S_{21}|$ occurs at a different frequency than resonant frequency of the coils [10]. Although this region has poor $|S_{21}|$ at a single operating frequency, implementing frequency tracking or adaptive impedance matching would enable higher $|S_{21}|$ in this region. $|S_{21}|$ drops below 0.9 for coil size ratios larger than 6.2 because k is weak between a large Tx coil and a much smaller Rx coil. However, the peak $|S_{21}|$ occurs at larger ratios as the distance increases beyond 6cm because $|S_{21}|$ decays slower for larger coil size ratios.

To verify that these simulated results are accurate for the full range of Tx coil sizes, we constructed three Tx coils and the 5.8cm Rx coil (Fig. 6). We designed the three Tx coils according to the recommended geometries for highest Q given by the optimization procedure. The three Tx to Rx coil size ratios are: 10:1 ($D_{O,TX1}$=56.5cm, N_1=3.4, p_1=7mm, w_1 = 2.05mm), 5:1 ($D_{O,TX2}$=28.5cm, N_2=8, p_2=7.5mm, w_2 = 1.63mm), and 2.25:1 ($D_{O,TX3}$=13cm, N_3=6, p_3=6mm, w_3 = 1.63mm). We used the VNA to extract several S_{21} datasets for a range of distances between the coils. Fig. 7 shows these experimental results plotted against the simulated results for the three coil size ratios indicated on Fig. 5.

The simulated and measured results match very closely for all sets of coils. The 10:1 ratio pair suffers from low coupling between the large Tx coil and small Rx coil, and therefore cannot achieve high $|S_{21}|^2$. However the coupling diminishes slower and the 10:1 ratio achieves its peak $|S_{21}|^2$ beyond 140cm. The 2.25:1 ratio suffers from over-coupling, and would require frequency tuning to accommodate for the reduced $|S_{21}|^2$ at close distances. The 5:1 ratio achieves high $|S_{21}|^2$ at close ranges, and a slower decrease in $|S_{21}|^2$ than the 2.25:1 ratio. The 5:1 ratio also follows the peak $|S_{21}|$ curve indicated on Fig. 5 most closely. For the proposed $0 < d < 140$cm range used in this example, the 5:1 ratio using TX_2 is optimal.

IV. Conclusion

This work provides simplified equations to model the parasitic components of flat, spiral coils used in WPT systems. The design procedure can facilitate the optimization of coil design for maximum WPT efficiency at the desired operating distance between coils for any given WPT application.

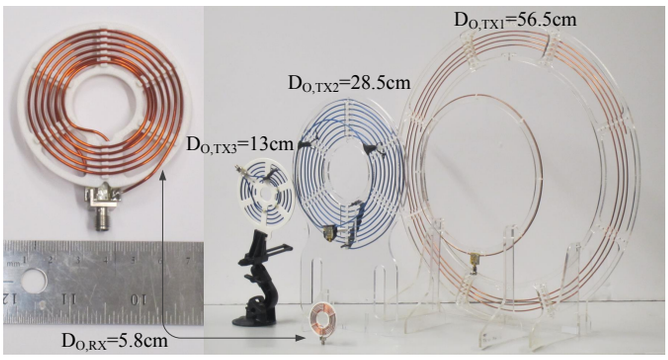

Fig. 6. Sets of Tx coils and Rx coils used for experimental measurements.

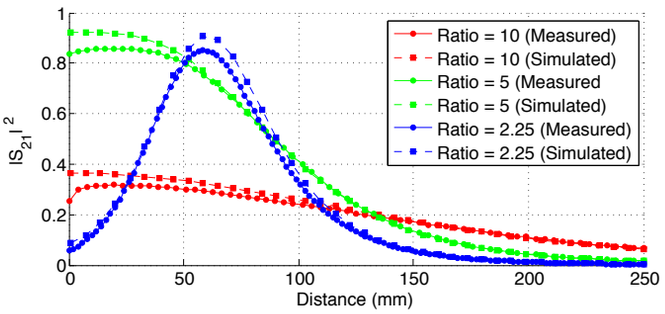

Fig. 7. Plot of measured and simulated $|S_{21}|$ for the coils from Fig. 6.

V. Acknowledgment

The authors thank Bosch for funding this work and members of the Sensor Systems Research Group for their help and invaluable feedback related to this work.

References

[1] A. P. Sample, D. A. Meyer, and J. R. Smith, "Analysis, experimental results, and range adaptation of magnetically coupled resonators for wireless power transfer," *Industrial Electronics, IEEE Transactions on*, vol. 58, no. 2, pp. 544–554, 2011.

[2] J. Ferreira, "Appropriate modelling of conductive losses in the design of magnetic components," in *Power Electronics Specialists Conference, 1990. PESC '90 Record., 21st Annual IEEE*, 1990, pp. 780–785.

[3] F. Grover, *Inductance calculations*, ser. Dover phoenix editions. Dover Publications, Incorporated, 2004.

[4] G. Grandi, M. Kazimierczuk, A. Massarini, and U. Reggiani, "Stray capacitances of single-layer air-core inductors for high-frequency applications," in *Industry Applications Conference, 1996. Thirty-First IAS Annual Meeting, IAS '96.*, vol. 3, 1996, pp. 1384–1388.

[5] S. Senjuti, "Design and optimization of efficient wireless power transfer links for implantable biotelemetry systems," Master's thesis, University of Western Ontario, May 2013.

[6] A. RamRakhyani, S. Mirabbasi, and M. Chiao, "Design and optimization of resonance-based efficient wireless power delivery systems for biomedical implants," *Biomedical Circuits and Systems, IEEE Transactions on*, vol. 5, no. 1, pp. 48–63, Feb 2011.

[7] S. Babic and C. Akyel, "Calculating mutual inductance between circular coils with inclined axes in air," *Magnetics, IEEE Transactions on*, vol. 44, no. 7, pp. 1743–1750, 2008.

[8] K. Kaiser, *Electromagnetic Compatibility Handbook*, ser. Electrical engineering handbook series. Taylor & Francis, 2004. [Online]. Available: http://books.google.com/books?id=nZzOAsroBIEC

[9] G. Lee, B. Waters, C. Shi, W. S. Park, and J. Smith, "Design considerations for asymmetric magnetically coupled resonators used in wireless power transfer applications," in *Radio and Wireless Symposium (RWS), 2013 IEEE*, Jan 2013, pp. 328–330.

[10] A. Sample, B. Waters, S. Wisdom, and J. Smith, "Enabling seamless wireless power delivery in dynamic environments," *Proceedings of the IEEE*, vol. 101, no. 6, pp. 1343–1358, 2013.